Observation of a novel ferromagnetic phase of Ho^{3+} in Ho/Lu superlattices

1993 J. Phys.: Condens. Matter 5 L481

(http://iopscience.iop.org/0953-8984/5/39/005)

J. Phys.: Condens. Matter 5 (1993) L481–L486. Printed in the UK

LETTER TO THE EDITOR

Observation of a novel ferromagnetic phase of Ho^{3+} in Ho/Lu superlattices

P P Swaddling†, D F McMorrow†, J A Simpson†, M R Wells†, R C C Ward† and K N Clausen‡

† Oxford Physics, Clarendon Laboratory, Parks Road, Oxford, OX1 3PU, UK
‡ Risø National Laboratory, Roskilde, DK 4000, Denmark

Received 25 May 1993, in final form 9 July 1993

Abstract. The magnetic structures of three Ho/Lu superlattices have been investigated using neutron diffraction. The low-temperature magnetic structure adopted by the Ho^{3+} moments is found to depend on the number n_{Ho} of atomic planes in a single block of Ho. For a sample with $n_{Ho} \simeq 40$ the moments form a basal-plane spiral down to the lowest temperatures investigated, whereas for two samples with $n_{Ho} \leqslant 20$ a phase transition occurs from a basal-plane spiral to a structure in which the Ho^{3+} moments within a single block align ferromagnetically.

One of the main attractions of using molecular beam epitaxy (MBE) to produce rare-earth superlattices is that it offers the opportunity to study the magnetic structure of a particular ion in an environment that is fundamentally different from that in the bulk metal, or that encountered in a random alloy. By carefully controlling the atomic deposition rate high-quality rare-earth superlattices in single-crystal form can be grown. In such an environment it is possible to examine the effects of strain and reduced dimensionality on the magnetism of a chosen element, and to alter these factors in a controlled way. In this letter we shall present the results of our neutron-diffraction data on a series of Ho/Lu superlattices. The magnetic structure of Ho/Y superlattices has recently been studied [1], and by comparing these data with our results we are able to establish any systematic differences between the two systems and to comment on their causes.

The magnetic structure of metallic Ho [2] is principally determined by two competing interactions: the indirect exchange and the crystal field. Below its Néel temperature of $T_N \simeq 133$ K and down to a temperature of 30 K, the Ho^{3+} moments form a basal-plane spiral in which the lowest-order term in the crystal field confines the moments to the basal plane, whilst the indirect exchange interaction requires that the moments in successive planes along the c axis rotate through a constant angle ψ_{Ho}. As the temperature is reduced further, the sixfold crystal-field anisotropy energy increases rapidly, causing the moments to move towards one of the six easy directions in the basal plane so as to form spin-slip structures [3,4]. These represent a compromise between the incommensurate wavevector required by the exchange and the commensurate structures favoured by the crystal field. At $\sim$ 18 K additional crystal-field terms cause a canting of 10° [5] of the moment out of the basal plane, with the dipolar interaction producing a ferromagnetic coupling of the c-axis components [6]. This is the cone phase, and it is characterized by a commensurate wavevector of $\frac{1}{6}c^*$; all of the moments are bunched in pairs around the easy directions, with a small ferromagnetic component along the c axis.

0953-8984/93/390481+06$07.50

As far as they may have a determining influence on the magnetic structure of the rare-earth superlattices, the physical properties of the two non-magnetic elements Y and Lu differ from each other in two important regards. The first simply relates to their ionic radii relative to that of Ho. The basal-plane lattice mismatch between Ho and Y is such that in producing an epitaxial interface between the two elements the Ho lattice experiences a tensile strain, with a consequent reduction in the *c*-axis lattice parameter; for Ho on Lu the basal-plane strain is compressive, and the lattice expands along *c*. The second is that the conduction electron susceptibility $\chi(q)$ of Y, as calculated by Liu *et al* [7], shows a strong peak, whereas that of Lu has a much weaker peak. Thus the indirect exchange interaction, which is mediated by the conduction electrons, couples the moments in adjacent Ho blocks more strongly across a block of Y than would be the case of an equivalent thickness of Lu. Previous studies of Dy/Y [8], Dy/Lu [9] and Er/Y [10] suggest that the strain is the more important of the two factors. It has been shown that Y has the effect of suppressing the transition from helical to magnetic ordering in Dy, while Lu produces an enhancement [9]. This has been interpreted as a change in the single-ion magnetoelastic term. In contrast the suppression of the *c*-axis moment in Er/Y superlattices has been attributed to a modification of the two-ion magnetoelastic constants. No significant changes in the observed magnetic structures have been attributed to the difference between the conduction electron susceptibilities of the non-magnetic spacers.

The Ho/Lu superlattices were grown with the chemical modulation direction along the crystallographic *c* axis using the MBE facility in the Clarendon Laboratory [12]. The series was designed to allow us to study the dependence of the magnetic structure on the length of the Ho block at constant Lu thickness. Three superlattices were grown with nominal Ho block lengths of 40, 20 and 10 atomic planes, punctuated by 15 atomic planes of Lu, with 50, 50 and 75 bilayer repeat units respectively. (The notation we shall follow is to specify the superlattice using the format $\{Ho_{40}/Lu_{15}\}_{50}$, etc.) The crystalline structure of the superlattices was studied using a combination of high-resolution x-ray diffraction techniques and modelling of the diffraction profile. This work established that the superlattices are single crystal in nature, with a higher degree of crystallographic perfection than is commonly found in rare-earth crystals grown by conventional means: the structural coherence length parallel to the growth direction was $\sim$ 2000 Å, the mosaic width of the (002) reflection was typically 0.2° and the interfaces between the two materials extended over three to four atomic planes. The actual structure of the three superlattices was found to be $\{Ho_{43}/Lu_{17}\}_{50}$, $\{Ho_{20}/Lu_{17}\}_{50}$ and $\{Ho_{10}/Lu_{17}\}_{75}$, with the Ho *c*-axis lattice parameters of 5.630(0.005), 5.635(0.005) and 5.660(0.005) Å respectively. Full details of the chemical structure will be published elsewhere [13].

The neutron-scattering experiments were performed at the DR3 reactor, Risø National Laboratory, Denmark using the triple-axis spectrometer TAS VII. With pyrolytic graphite monochormator and analyser crystals, and with reactor-to-detector collimation of 28′-40′-40′-140′, the wavevector resolution along [00*l*] was typically 0.011 $Å^{-1}$ (FWHM) for 5 meV neutrons. Second-order contamination of the incident beam was reduced by the use of a cooled Be filter. The samples were mounted with the $[1\bar{2}0]$ reciprocal lattice vector perpendicular to the scattering plane, in a closed-cycle He cryostat. Scans of the neutron wavevector transfer Q were performed, as a function of temperature, along [00*l*] and [10*l*]. The former provides information on the components of the magnetic moments in the basal plane, whereas the latter is sensitive to the components along both [00*l*] and $[1\bar{2}0]$.

We will start our presentation of the neutron-scattering data by considering the results from the sample of nominal composition $\{Ho_{40}/Lu_{15}\}_{50}$. At temperatures above 133 K, scans of the wavevector transfer along [00*l*] revealed the presence of the (002) nuclear

Bragg peak (at $Q \simeq 2.25$ Å^{-1}), with satellites characteristic of the superlattice chemical modulation. Below this temperature, an additional group of peaks became evident either side of the nuclear scattering, as shown in figure 1. The intensity of these peaks increased rapidly with decreasing temperature, while at the same time they moved closer to the nuclear scattering. These peaks are therefore magnetic in origin. From the fact that no extra scattering was observed at the (100) Bragg peak, we can conclude that below 133 K and down to a temperature of 12 K, the Ho^{3+} moments form a spiral confined to the hexagonal basal plane. An important additional feature of the magnetic scattering displayed in figure 1 is that within one group there are well defined superlattice peaks. This shows that the ordering of the Ho^{3+} moments is coherent across the Lu layer. The magnetic correlation length deduced from the width of the peaks is ~ 400 Å, i.e. greater than two bilayer units.

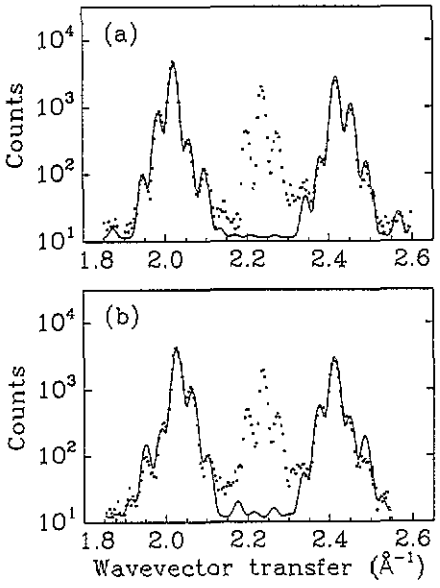

Figure 1. The measured intensity of the neutron scattering from the $\{Ho_{40}/Lu_{15}\}_{50}$ superlattice in a scan of the wavevector transfer Q along [00l] at (*a*) 30 K and (*b*) 12 K. The full curves represent the results of a least-squares fit of our scattering model to the data. The parameters of the fit are: (*a*) $\psi_{Ho} = 33.0(1)^\circ$ and $\psi_{Lu} = 40.0(1)^\circ$; (*b*) $\psi_{Ho} = 29.8(1)^\circ$ and $\psi_{Lu} = 39.3(1)^\circ$. The peaks at $Q \simeq 2.25$ Å^{-1} arise from nuclear scattering processes.

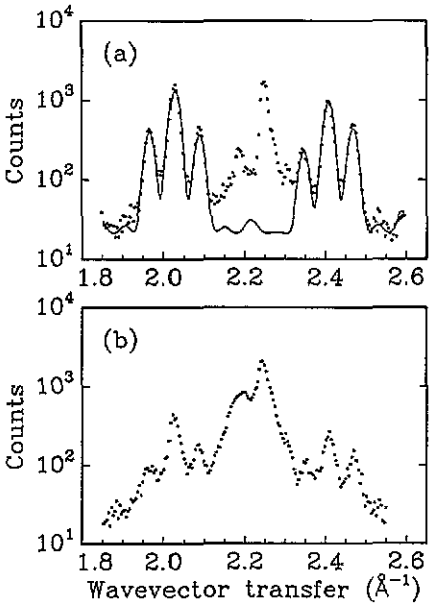

Figure 2. The measured intensity of the neutron scattering from the $\{Ho_{20}/Lu_{15}\}_{50}$ superlattice in a scan of the wavevector transfer along [00l] at (*a*) 30 K and (*b*) 12 K. The full curve in (*a*) represents the results of a least-squares fit of our scattering model to the data and is described in the text. The parameters of the fit are $\psi_{Ho} = 30.9(1)^\circ$ and $\psi_{Lu} = 40.4(1)^\circ$.

For temperatures between its ordering temperature of $T_N \simeq 130$ K and 30 K, the results from the $\{Ho_{20}/Lu_{15}\}_{50}$ superlattice are qualitatively similar to those described above and an example is shown in figure 2(*a*). Thus, in this temperature interval the Ho^{3+} moments in this superlattice also form a basal-plane spiral. On further cooling there was a dramatic

change in the distribution of the scattered intensity, as depicted in figure 2(*b*). A broad peak appeared at $Q \simeq 2.20$ Å^{-1} close to the (002) nuclear peak, with a concomitant reduction in the scattering in the spiral sidebands. This indicates that below $T_C \simeq 30$ K, there is a mixture of two magnetic phases: some of the moments still form a basal-plane spiral, but in addition a new phase develops in which the Ho^{3+} moments within a single Ho block are ferromagnetically coupled in the basal plane. The onset of the ferromagnetic order is also accompanied by an increase in scattering at the (100) peak. Because of the geometric selection rule for magnetic scattering, we are presently unable to determine whether this increase arises from a tilting of the moments out of the basal plane, or from the formation of ferromagnetic domains along each of the six equivalent easy directions in the basal plane. Further experiments are in progress to distinguish between these two cases. The $\{Ho_{10}/Lu_{15}\}_{75}$ superlattice also displayed the same sequence of phase transitions, except that in this case the transition to the ferromagnet occurs at an elevated temperature of 40(5) K. We will return to a more detailed discussion of the nature of this phase after we have considered the data from the spiral phase of the three superlattices.

Without recourse to fitting the intensity of the magnetic peaks it is not possible to extract separately the individual turn angles through the Ho and Lu. The method we adopted in fitting the data was the same as used in our previous study of Ho/Y [1]. We assume that there is a helix through both the Ho and the Lu, with different turn angles ψ_{Ho} and ψ_{Lu}, but with no moment at the Lu sites. In the interfacial region the turn angle varies smoothly between the two. Typical fits of the scattering from this simple model are represented by the full curves in figures 1 and 2(*a*), where it can be seen that the model provides a good description of the data over several decades of intensity.

The results of this analysis for the $\{Ho_{40}/Lu_{15}\}_{50}$ and $\{Ho_{20}/Lu_{15}\}_{50}$ superlattices are summarized in figure 3, in which a number of trends are apparent. In the spiral phase, the effective turn angle through the Lu layer has a value of 40(1)° per layer, independent of temperature, and has the same value for all three superlattices. This is significantly lower than either the value found in studies of Dy/Lu [9], or the value extrapolated from dilute Lu alloys of 48° [14]. The reason for this discrepancy is not known. In contrast, the turn angle through the Ho is strongly temperature dependent. In the case of the $\{Ho_{40}/Lu_{15}\}_{50}$ superlattice the temperature dependence of ψ_{Ho} is close to that found in bulk Ho. At a given temperature, ψ_{Ho} lies slightly below its bulk value, but locks into a value of 30° per layer at low temperature. As far as we can ascertain, this is not the cone phase because the moment remains confined to the basal plane down to a temperature of 12 K. For the two other superlattices, it is found that at temperatures just above the transition to the ferromagnetic phase, $\psi_{Ho} \simeq 30°$. Thus, it appears that this phase transition can only proceed after the spiral becomes commensurate with a wavevector of $q = \frac{1}{6}c^*$. The final trend we note is that at a given temperature the difference between the value of ψ_{Ho} in the bulk and in the superlattice increases as the thickness of the Ho block decreases.

We will now return to the nature of the ferromagnetic phase observed in the $\{Ho_{20}/Lu_{15}\}_{50}$ and $\{Ho_{10}/Lu_{15}\}_{50}$ superlattices. We have extracted the magnetic scattering from the low-temperature data (figure 2(*b*)) by subtraction of the nuclear scattering measured just above the transition (figure 2(*a*)). The difference spectrum is displayed in figure 4. The resulting scattering has a series of peaks positioned around (002) ($Q \simeq 2.25$ Å^{-1}), with a separation corresponding to four bilayer repeat units, a value that indicates a quadrupling of the unit cell along *c*. There are several candidate structures that are compatible both with this observation and the symmetry, but our data do not allow us to make a unique selection.

We now briefly compare these results with the recent work on Ho/Y superlattices. Our results demonstrate that the substitution of Lu for Y has a profound effect on the observed

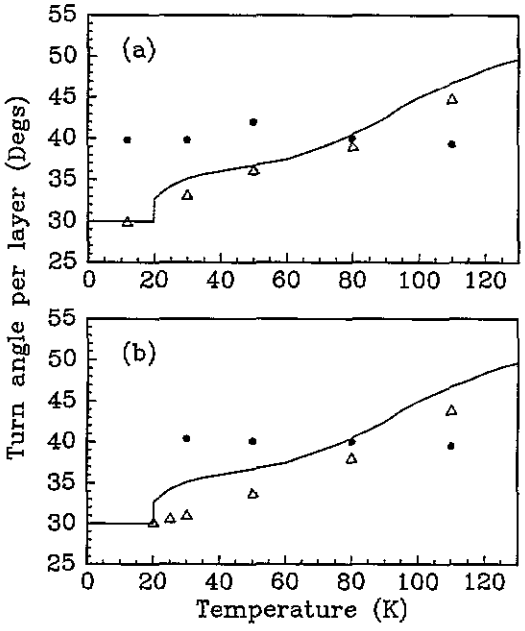

Figure 3. The temperature dependence of the turn angle, ψ_{Ho} in Ho (open triangles) and the turn angle, ψ_{Lu} in Lu (filled circles) for the (*a*) $\{Ho_{40}/Lu_{15}\}_{50}$ and (*b*) $\{Ho_{20}/Lu_{15}\}_{75}$ superlattices. The full curves are the turn angle measured in bulk Ho [3].

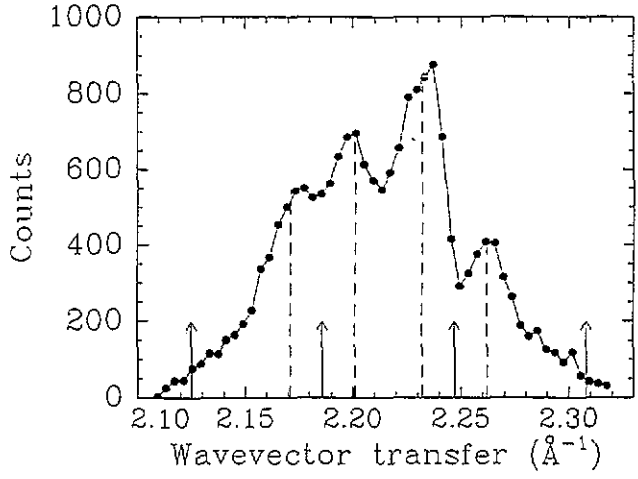

Figure 4. The difference spectrum of the data shown in figures 2(*b*) and 2(*a*) for the $\{Ho_{20}/Lu_{15}\}_{50}$ superlattice. The scattering is magnetic in origin and the spacing between the peaks corresponds to a structure with a unit cell of four bilayer repeats along c. The arrows indicate the positions of the nuclear peaks before the subtraction and the broken lines lie at $Q = 2.247 + (2n + 1)\Delta Q$, where $\Delta Q = \pi/2\Lambda$ and Λ is the bilayer repeat length in Å.

magnetic structure adopted by the Ho^{3+} moments in a superlattice. In particular, there are two significant differences. First, at a given temperature in the helical phase, ψ_{Ho} in Ho/Y is always greater than the value found in Ho/Lu and is a continuously decreasing function of the Ho *c*-axis lattice parameter. This will be dealt with in more detail in a forthcoming publication. The second, and more dramatic, difference between the two Ho-based superlattices, is that for thin blocks of Ho, a transition to a ferromagnet occurs

in Ho/Lu, whereas the corresponding Ho/Y superlattices always form a basal-plane spiral. It has been shown by Bohr *et al* [16] that, for a free-standing Ho block, the difference in energy between the spiral and ferromagnetic phases decreases with the block length, and that the latter phase becomes favourable for blocks of nine atomic planes or less. However, the calculation does not take into account any dependence of the indirect exchange parameters on the strain, nor any interaction between adjacent Ho blocks. Within these limitations, and recognizing that the strain appears to be responsible for the onset of the new phase, we find it difficult to comment on the validity of such a calculation. We simply observe that it is the samples in which the Ho is under the greatest tensile strain that we find a ferromagnetic structure.

To summarize, we have found that the strain introduced by the epitaxial growth plays a crucial role in determining the magnetic structure. The Ho turn angle at a given temperature depends on the value of the c-axis lattice parameter for Ho, and two highly strained samples exhibit a low-temperature transition to ferromagnets. The observation of this phase transition in Ho represents one of the best examples of how the process of MBE may be used to create novel magnetic structures.

We have benefited from many useful discussions with R A Cowley, A R Mackintosh and J Jensen. We would like to thank the technical staff at Risø for their help in performing these experiments. Financial support for the work at Risø was provided by the EC under the Large Scale Facility Programme. The work in Oxford was funded by the Science and Engineering Research Council.

References

[1] Jehan D A, McMorrow D F, Cowley R A, Ward R C C, Wells M R, Hagmann N and Clausen K N 1993 *Phys. Rev.* B at press
[2] Koehler W C, Cable J W, Wilkinson M K and Wollan F O 1966 *Phys. Rev.* **151** 414
[3] Gibbs D, Moncton D E, D'Amico K L and Bohr J and Grier B H 1985 *Phys. Rev. Lett.* **55** 234
[4] Cowley R A and Bates S 1988 *J. Phys. C: Solid State Phys.* **21** 4113
[5] Koehler W C, Cable J W, Wilkinson M K and Wollan E O 1966 *Phys. Rev.* **151** 414
[6] Larsen C C, Jensen J and Mackintosh A R 1987 *Phys. Rev. Lett.* **59** 712
[7] Liu S H, Gupta R P, Sinha S K 1971 *Phys. Rev.* B **4** 1100
[8] Erwin R W, Rhyne J J, Salamon M B, Borchers J, Sinha S K, Du R, Cunningham J E and Flynn C P 1987 *Phys. Rev.* B **35** 6808
[9] Beach R S, Borchers J A, Matheny A, Erwin R W, Salamon M B, Everitt B, Pettit K, Rhyne J J and Flynn C P 1993 *Phys. Rev. Lett.* **70** 3502
[10] Borchers J A, Salamon M B, Erwin R W, Rhyne J J, Du R and Flynn C P 1991 *Phys. Rev.* B **43** 3123
[11] Kawano S, Achiwa N, Onodera A, Nakai Y and Lebech B to be published
[12] Wells M R, Ward R C C, Hagmann N, Swaddling P P, McMorrow D F and Jehan D A to be published
[13] Swaddling P P and McMorrow D F to be published
[14] Child H R, Koehler W C, Wollan E D and Cable J W 1965 *Phys. Rev.* **138** A1655
[15] Umbayashi H, Shirane G and Frazer B C 1967 *Phys. Rev.* **165** 688
[16] Bohr J, Gibbs D, Axe J D, Moncton D E, D'Amico K L, Majkrzak C F, Kwo J, Hong M, Chien C L and Jensen J 1989 *Physica* B **159** 93